PROGRESSING TORSIONAL LOADS ALONG A BORE IN AN ELASTIC MEDIUM

R. PARNES

Department of Solid Mechanics, Materials and Structures, School of Engineering, Tel-Aviv University, Ramat-Aviv, Israel

Abstract—A torsional line load applied along a transverse circle travels in the axial direction along the interior of a cylindrical bore in an infinite elastic medium. The line load moves with a constant velocity V which is either greater or less than the velocity of the equivoluminal waves which are found to propagate in the medium. The resulting superseismic and subseismic responses are derived as steady-state solutions which do not change in a coordinate system which, attached to the applied torsional loads, moves with velocity V. Displacement and stress components are obtained for points throughout the medium. In the superseismic case, a sharp S-wave front exists and the behavior at this front is investigated. Numerical results are presented for the displacements and stresses throughout the medium for both superseismic and subseismic cases.

1. INTRODUCTION

The problem of elastic bodies subjected to moving loads has received considerable attention in recent years. A comprehensive summary of such problems is given in [1]. Among the first investigations were the solutions given by Sneddon[2] and by Cole and Huth[3] who considered the two-dimensional problem of a progressing normal line load travelling with constant velocity on the surface of a half-space. The problem of a line load travelling with velocity V in the axial direction along the interior of a circular bore contained in an elastic medium was later considered[4]. In general both P- and S-waves were excited by the application of such loads. Because of the complexity of the geometry, only the superseismic case (that where V is greater than the propagation velocity of either P- or S-waves) was investigated, and the displacement and stress quantities were evaluated only on the cavity surface.

In the present paper, the problem considered is that of a torsional line load travelling with velocity V along the interior of a cylindrical bore in an elastic medium. In this case, only shear waves, travelling with velocity c_s are propagated in the medium.

Disregarding initial conditions at far distances, a steady state solution is obtained in a travelling coordinate system which is attached to the applied torsional load.

Solutions are derived both for the superseismic ($V/c_s > 1$) and subseismic ($V/c_s < 1$) cases. Expressions for the displacements and stresses are obtained throughout the medium, and the behavior and jumps at the wave front, in the superseismic case, is investigated. For this case, the peak displacements which occur at the wave fronts are shown to be expressible by means of a simple algebraic relation. Numerical results are presented for typical superseismic and subseismic cases.

2. GENERAL FORMATION

Consider a cylindrical bore of radius $r = a$ in a linear elastic isotropic medium referred to a fixed coordinate system ($\bar{r}$, $\bar{\theta}$, $\bar{z} = a\xi$) whose origin lies on the axis of the bore (Fig. 1). A torsional line load, applied along the circle at $\bar{z} = -Vt$ progresses along the interior of the bore with velocity V such that the stresses on the boundary are given by

$$\sigma_{r\theta} = P\delta(\bar{z} + Vt)$$

$$\sigma_{rz} = 0, \quad \sigma_{rr} = 0 \tag{1}$$

where δ is the Dirac-delta function.

The displacement

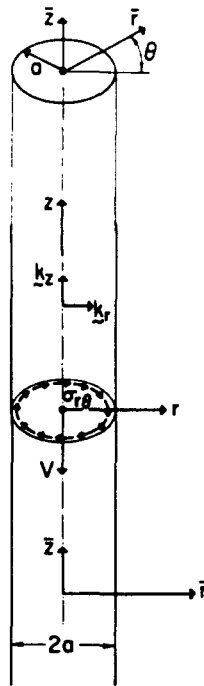$$\bar{u}(\bar{r}, \bar{\theta}, \bar{z}, t) = w\bar{k}_r + v\bar{k}_\theta + u\bar{k}_z \tag{2}$$

Fig. 1. Geometry of the problem.

must satisfy the equation of motion for the elastic medium

$$\mu \nabla^2 \bar{u} + (\lambda + \mu)\nabla\nabla \cdot \bar{u} = \rho_D \ddot{\bar{u}} \tag{3}$$

where μ and λ are the Lamé constants and ρ_D is the mass density.

To determine the steady-state solution, we introduce a non-dimensional coordinate system $(\rho = r/a, \theta, \xi = z/a)$ which is attached to the circle of load application and travels with velocity V along the longitudinal axis. Accordingly, the two coordinate systems are related by the Galilean transformation

$$\rho = \bar{r}/a, \quad \theta = \bar{\theta}, \quad \xi = z/a = \frac{1}{a}(\bar{z} - Vt). \tag{4}$$

The equation of motion, eqn (3) referred to the moving coordinate system becomes

$$\mu \nabla^2 \bar{u} + (\lambda + \mu)\nabla\nabla \cdot \bar{u} = \rho_D \frac{V^2}{a^2} \frac{\partial^2 \bar{u}}{\partial \xi^2} \tag{5}$$

where now

$$\bar{u}(r, \theta, \xi) = w(r, \theta, \xi)\bar{k}_r + v(r, \theta, \xi)\bar{k}_\theta + u(r, \theta, \xi)\bar{k}_z \tag{6}$$

and

$$\nabla \equiv \frac{1}{a}\left[\frac{\partial}{\partial \rho}\bar{k}_r + \frac{1}{\rho}\frac{\partial}{\partial \theta}\bar{k}_\theta + \frac{\partial}{\partial \xi}\bar{k}_z\right]. \tag{7}$$

The corresponding boundary conditions, at $\rho = 1$ from eqn (1), are

$$\sigma_{r\theta} = \frac{P}{a}\,\delta(\xi), \quad \sigma_{rr} = \sigma_{rz} = 0. \tag{8}$$

For this axisymmetric case, solutions satisfying eqn (5) and the boundary conditions are

$$v = v(\rho, \xi), \quad u = w = 0. \tag{9}$$

Equation (5) then reduces to the scalar equation

$$c_s^2 \nabla^2 v(\rho, \xi) = \frac{V^2}{a^2} \frac{\partial^2 v}{\partial \xi^2} \tag{10}$$

where

$$c_s = \sqrt{(\mu/\rho_D)} \tag{11}$$

is the propagation velocity of shear waves in the medium. Written explicitly, eqn (10) becomes

$$\frac{\partial^2 v}{\partial \rho^2} + \frac{1}{\rho} \frac{\partial v}{\partial \rho} - \frac{1}{\rho^2} v - m^2 \frac{\partial^2 v}{\partial \xi^2} = 0 \tag{12}$$

where

$$m^2 = M^2 - 1, \tag{13a}$$

with

$$M = V/c_s \tag{13b}$$

being the Mach number with respect to the S-wave velocity.
The stresses, obtained from the stress-strain relations

$$\tilde{\sigma} = \lambda \nabla \cdot \vec{u} I + \mu [\nabla \vec{u} + \vec{u} \nabla], \tag{14}$$

become

$$\sigma_{r\theta} = \frac{\mu}{a} \left(\frac{\partial v}{\partial \rho} - \frac{v}{\rho} \right) \qquad \text{(a)}$$

$$\sigma_{\theta z} = \frac{\mu}{a} \frac{\partial v}{\partial \xi} \qquad \text{(b)} \tag{15}$$

$$\sigma_{rr} = \sigma_{\theta\theta} = \sigma_{rz} = \sigma_{zz} = 0 \qquad \text{(c)}$$

The last two boundary conditions of eqn (8) are identically satisfied while the remaining boundary condition can be expressed as

$$\left. \frac{\partial v}{\partial \rho} - \frac{v}{\rho} \right|_{\rho=1} = \frac{P}{\mu} \delta(\xi). \tag{16}$$

Equation (12) must thus be solved subject to the boundary condition of eqn (16). It is recognized that the character of the solution of eqn (12) depends on the sign of m: for $V/c_s > 1$, $(m^2 > 0)$ the solution corresponds to the superseismic case while for $V/c_s < 1$, $(m^2 < 0)$ the subseismic solution is obtained. Each of these cases must be treated separately.

3. SOLUTION:SUPERSEISMIC CASE, $V/c_s > 1$

For $m^2 > 0$ which corresponds to the superseismic case, it is clear that eqn (12) is hyperbolic and that a sharp jump exists at the wave front (Fig. 2). The wave front for the steady-state conditions can be established simply from geometric considerations.
Letting (ρ_f, ξ_f) denote the coordinates at all points along the wave front, and noting that

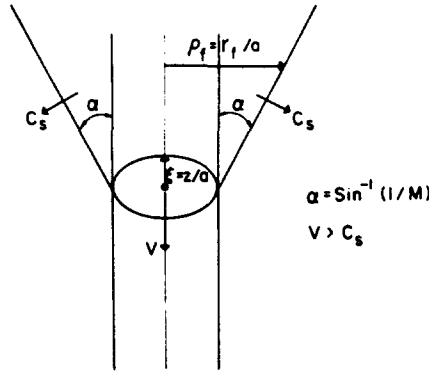$$\sin \alpha = c_s/V = 1/M \tag{17a}$$

Fig. 2. Superseismic case.

and

$$\tan \alpha = (\rho_f - 1)/\xi_f, \tag{17b}$$

the equation for the wave front is given by

$$\xi_f = m(\rho_f - 1). \tag{18}$$

Thus, the wave front appears as a conically shaped front inclined at an angle $\alpha = \sin^{-1}(1/M)$ to the longitudinal axis. Ahead of this wave front there exists a quiescent state. Since, in particular, this is true for $\xi < 0$, the Laplace transform

$$\bar{f}(s) = \mathscr{L}[f(\xi)] = \int_0^\infty f(\xi)e^{-s\xi}\mathrm{d}\xi, \tag{19a}$$

with inversion

$$f(\xi) = \frac{1}{2\pi i} \int_{\gamma-i\infty}^{\gamma+i\infty} \bar{f}(s)e^{s\xi}\mathrm{d}s \tag{19b}$$

is appropriate.

Applying the transform to eqn (12) we obtain the governing equation for $\bar{v}(\rho, s)$:

$$\frac{\partial^2 \bar{v}}{\partial \rho^2} + \frac{1}{\rho^2}\frac{\partial \bar{v}}{\partial \rho} - (m^2 s^2 + 1/\rho^2)\bar{v} = 0. \tag{20}$$

The non-vanishing transformed stresses throughout the medium are then

$$\bar{\sigma}_{r\theta}(\rho, s) = \frac{\mu}{a}\left(\frac{\partial \bar{v}}{\partial \rho} - \frac{\bar{v}}{\rho}\right) \tag{21a}$$

$$\bar{\sigma}_{z\theta}(\rho, s) = \frac{\mu s}{a}\bar{v}(\rho, s) \tag{21b}$$

and consequently the transformed boundary condition becomes

$$\left.\frac{\partial \bar{v}}{\partial \rho} - \frac{\bar{v}}{\rho}\right|_{\rho=1} = \frac{P}{\mu}. \tag{22}$$

Solutions of eqn (20) which decay as $\rho \to \infty$ are

$$\bar{v}(\rho, s) = A(s)K_1(ms\rho) \tag{23}$$

where $A(s)$ is an arbitrary constant and K_n is the modified Bessel function of the second kind of order n.

Substitution of eqn (23) in eqn (22) yields

$$A(s) = -\frac{P}{ms\mu}\frac{1}{K_2(ms)} \tag{24}$$

and hence

$$\bar{v}(\rho, s) = -\frac{P}{ms\mu}\frac{K_1(ms\rho)}{K_2(ms)}. \tag{25}$$

The resulting transformed stresses, by eqn (21), are then

$$\bar{\sigma}_{r\theta}(\rho, s) = \frac{P}{a}\frac{K_2(ms\rho)}{K_2(ms)} \tag{26a}$$

$$\bar{\sigma}_{\theta z}(\rho, s) = -\frac{P}{ma}\frac{K_1(ms\rho)}{K_2(ms)}. \tag{26b}$$

The displacement and stress components are now obtained by inversion using the Bromwich integral, eqn (19b):

$$\frac{\mu v}{P}(\rho, \xi) = -\frac{1}{2\pi i}\int_{\gamma-i\infty}^{\gamma+i\infty}\frac{K_1(ms\rho)}{msK_2(ms)}e^{s\xi}ds \tag{27a}$$

$$\frac{a\sigma_{r\theta}}{P}(\rho, \xi) = \frac{1}{2\pi i}\int_{\gamma-i\infty}^{\gamma+i\infty}\frac{K_2(ms\rho)}{K_2(ms)}e^{s\xi}ds \tag{27b}$$

$$\frac{a\sigma_{\theta z}}{P}(\rho, \xi) = -\frac{1}{2\pi i}\int_{\gamma-i\infty}^{\gamma+i\infty}\frac{K_1(ms\rho)}{mK_2(ms)}e^{s\xi}ds \tag{27c}$$

The above integrals may be evaluated by contour integration upon extending into the complex plane (Fig. 3). Because of the multi-valued nature of the K_n functions, a branch cut emanating from a branch point at the origin is taken along the negative real axis. The resulting contours are as shown in (Fig. 3) where the circular arcs BC and FA have radius $R \to \infty$.
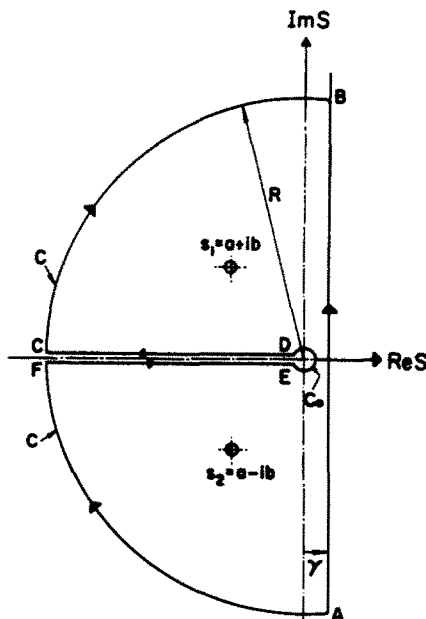

Fig. 3. Integration contour.

By the residue theorem, the above integrals may be expressed, in general, as

$$I_{()} = 2\pi i \sum_j \text{Res}_{()} + I_{B_{()}} + I_{o_{()}} + I_{C_{()}}$$

where, written symbolically

$I_{()} = \int_A^B \bar{f}(\rho, s)e^{s\xi}ds$ represents the desired Bromwich integral,

$\sum_j \text{Res}_{()}[\bar{f}(\rho, s); s_j]$ represents the sum of residues at points $s = s_j$

$I_{B_{()}} = \int_F^E + \int_D^C$ represents the branch integrals

$I_{o_{()}} = \oint_{C_o}$ represents the contribution from the branch point

and

$I_{C_{()}} = \int_A^F + \int_C^B$ represents the contribution along the large circular arcs

as $R \rightarrow \infty$.

In the above (v) denotes the displacement and $(r\theta)$ and (θz) denote the stress component quantities $\sigma_{r\theta}$ and $\sigma_{\theta z}$ respectively.

The residues, in all cases, are due to simple poles which are located at the points defined by the roots $s = s_j$ of $K_2(ms) = 0$, and which are given by[5]

$$ms_{1,2} = -1.2813738 \pm 0.4294850i. \tag{28}$$

The residues of the expressions appearing in eqns (27) are obtained by considering the integrands as simple quotients. From the known property of the Bessel function[6]

$$K_2'(z) = -\frac{2}{z}K_2(z) - K_1(z) \tag{29}$$

and the recursion formulae of the Bessel functions, the residue for the displacement v at s_j becomes

$$\text{Res}_{(v)}[\bar{f}, s = s_j] = -\frac{K_1(ms_j\rho)}{m^2 s_j K_1(ms_j)} e^{s_j\xi}. \tag{30}$$

Noting that the poles s_j lie at complex conjugate points and recalling that[7]

$$K_n(\bar{s}) = \overline{K_n(s)}, \tag{31}$$

the sum of the residues is given by

$$\sum_{j=1}^2 \text{Res}_{(v)}[\bar{f}, s = s_j] = -\frac{2Re}{m^2}\left\{\frac{K_1(ms_1\rho)e^{s_1\xi}}{s_1 K_1(ms_1)}\right\}, \quad \rho \geq 1 \tag{32a}$$

where Re denotes the real part of a complex function.

Similarly, the residues for the stresses $\sigma_{r\theta}$ and $\sigma_{\theta z}$ become

$$\sum_{j=1}^2 \text{Res}_{(\theta r)}[\bar{f}, s = s_j] = -\frac{2}{m}Re\left\{\frac{K_2(ms_1\rho)e^{s_1\xi}}{K_1(ms_1)}\right\}, \quad \rho > 1 \tag{32b}†$$

---

†It is noted, from eqn (27b) that a simple pole exists at $s = s_j$ for $\rho > 1$. However, when $\rho = 1$, the singularity at $s = s_j$ is removable and hence no residue can exist.

$$\sum_{j=1}^{2} \text{Res}_{(\theta z)}[\bar{f}, s = s_j] = -\frac{2}{m^2} \text{Re} \left\{ \frac{K_1(ms_1\rho)e^{s_1\xi}}{K_1(ms_1)} \right\}, \quad \rho \geq 1. \tag{32c}$$

The branch integrals are determined by letting $s = -\zeta$ ($\zeta > 0$, real). Using the relation[6]

$$K_n(\eta e^{\pm i\pi}) = (-1)^n K_n(\eta) \pm i\pi I_n(\eta), \tag{33}$$

where $I_n(\eta)$ is the modified Bessel function of the first kind of order n, after some algebraic manipulation, and upon noting the complex conjugate nature of the functions along the upper and lower branches, the following expression for the displacements and stress components are established:

$$I_{B_{(r)}} = -\frac{2\pi i}{m} \int_0^\infty \frac{G_1(m\zeta,\rho)}{\zeta D(m\zeta)} e^{-\zeta\xi} d\zeta \tag{34a}$$

$$I_{B_{(r\theta)}} = 2\pi i \int_0^\infty \frac{G_2(m\zeta,\rho)}{D(m\zeta)} e^{-\zeta\xi} d\zeta \tag{34b}$$

$$I_{B_{(\theta z)}} = \frac{2\pi i}{m} \int_0^\infty \frac{G_1(m\zeta,\rho)}{D(m\zeta)} e^{-\zeta\xi} d\zeta \tag{34c}$$

where

$$G_n(m\zeta,\rho) = I_n(m\rho\zeta)K_2(m\zeta) - (-1)^n K_n(m\rho\zeta)I_2(m\zeta), \quad n = 1,2 \tag{35a}$$

and

$$D(\zeta) = K_2^2(m\zeta) + \pi^2 I_2^2(m\zeta). \tag{35b}$$

The contributions I_0 and I_c along c_0 at the origin and along the large circular arcs are found using the small circle lemma and large circle lemma respectively[8]. The contribution I_0 is found to vanish in all cases. To evaluate I_c, the functions are first represented by their asymptotic expansion.

From the asymptotic expansion of the Bessel function[6],

$$K_n(z) \approx \sqrt{\left(\frac{\pi}{2z}\right)} e^{-z} \left\{ 1 + \frac{a_n}{z} + \frac{b_n}{z^2} + \ldots \right\} \tag{36a}$$

where

$$a_n = \frac{4n^2 - 1}{8}, \quad b_n = \frac{(4n^2 - 1)(4n^2 - 9)}{128}, \tag{36b}$$

and hence along the large circular arcs the ratios appearing in the integrands of eqn (27) are either of the form

$$\lim_{|s| \to \infty} \frac{K_n(ms\rho)}{K_2(ms)} e^{s\xi} = \lim_{|s| \to \infty} \{\rho^{-1/2} e^{[\xi - m(\rho-1)]s}\} \quad n = 1,2 \tag{37a}$$

or

$$\lim_{|s| \to \infty} \frac{K_1(ms\rho)}{sK_2(ms)} e^{s\xi} = \lim_{|s| \to \infty} \left\{\rho^{-1/2} \frac{e^{[\xi - m(\rho-1)]s}}{s}\right\}. \tag{37b}$$

Since the contours lie in the quadrants for which $\text{Re}\{s\} < 0$, it follows that the integrals along the arcs can be convergent only if

$$\xi - m(\rho - 1) > 0, \tag{38}$$

i.e. the Laplace transform solution is valid only in this domain, which comparing with eqn (18), is seen to lie behind the wave front.

From eqn (27b,c) and eqn (37a), the large circle contributions for the stress quantities are

$$I_c \sim \rho^{-1/2} \int_c e^{[\xi - m(\rho - 1)]s} \, ds \tag{39}$$

where c can now be considered as a single circular contour extending from A to B. Since the integrand appearing in eqn (39) is analytic everywhere in the complex plane, the contour may be deformed, according to the Cauchy theorem, and hence

$$I_c \sim \rho^{-1/2} \int_{\gamma - i\infty}^{\gamma + i\infty} e^{[\xi - m(\rho - 1)]s} \, ds. \tag{40}$$

Noting that [9]

$$\int_{\gamma - i\infty}^{\gamma + i\infty} e^{s\xi} ds = 2\pi i \delta(\xi), \tag{41}$$

and using the property of the Laplace transform

$$\mathcal{L}[f(z - z_0)] = e^{-sz_0} \bar{F}(s), \tag{42}$$

it follows that

$$\int_c \frac{K_n(m\rho s)}{K_2(ms)} e^{-s\xi} ds = 2\pi i \rho^{-1/2} \delta[\xi - m(\rho - 1)], \quad n = 1, 2. \tag{43}$$

Consequently

$$I_{c_{(r\theta)}} = 2\pi i \rho^{-1/2} \delta[\xi - m(\rho - 1)] \tag{44a}$$

$$I_{c_{(\theta z)}} = \frac{-2\pi i \rho^{-1/2}}{m} \delta[\xi - m(\rho - 1)]. \tag{44b}$$

We thus note that the large circle contributions describe the behavior at the wave front, which for the case of the stress components are expressed as Dirac-delta functions.

The large circle contributions to the displacement v can be treated similarly, yielding a particularly interesting result. From eqn (27a) and (37b),

$$I_{c(v)} = \frac{\rho^{-1/2}}{m} \int_c \frac{e^{[\xi - m(\rho - 1)]s}}{s} \, ds \tag{45}$$

which, by the large circle lemma vanishes for $\xi > m(\rho - 1)$. However, at the wave front

$$I_{c(v)} = \frac{\rho^{-1/2}}{m} \int_c \frac{ds}{s} = -\rho^{-1/2} \pi i / m \tag{46a}$$

and consequently

$$I_{c(v)} = \begin{cases} -i\pi \rho^{-1/2}/m, & \rho = \rho_f \\ 0 & \rho \neq \rho_f. \end{cases} \tag{46b}$$

The quantity

$$\frac{\mu v(\rho_f, \xi)}{P} = \frac{\rho_f^{-1/2}}{2m} \tag{47}$$

is thus seen to represent precisely half the jump in displacement which occurs at the wave front. Hence, since the displacements are zero ahead of the front, we obtain a simple expression for the displacement immediately behind the front; viz.

$$\frac{\mu v(\bar{\rho}_f,\xi)}{P} = -\frac{\rho_f^{-1/2}}{m}. \tag{48}$$

A similar description of the behavior at wave fronts has been observed in previous investigations[10].

From the above analysis, it is possible to verify the Rankine-Huginiot relation existing at the front[11],

$$[\rho \dot{v} \bar{V}_n + \bar{T}_n] = 0, \tag{49}$$

where [ ] denotes the jump, $\dot{v}$ is the particle velocity, V_n is the wave propagation velocity normal to the front and $\bar{T}_n$ is the traction existing at the front. Noting that here $V_n = c_s$, by eqns (4) and (13b),

$$\dot{v} = \frac{dv}{dz}\frac{dz}{dt} = -V\frac{dv}{dz} = -c_s M\frac{dv}{dz}, \tag{50}$$

and from eqn (11), eqn (49) becomes

$$\left[-\frac{\mu M}{a}\frac{dv}{d\xi} + \sigma_{n\theta}\right] = 0 \tag{51}$$

where $\sigma_{n\theta}$ is the circumferential shear stress component at the wave front. Hence, in transform space,

$$\left[-\frac{\mu M}{a}s\bar{v} + \bar{\sigma}_{n\theta}\right] = 0. \tag{52}$$

From a simple analysis of a wedge-shaped element of the medium in the region of the wave front,

$$\sigma_{n\theta} = -\frac{1}{M}(m\sigma_{r\theta} - \sigma_{\theta z}). \tag{53a}$$

However, using eqn (27b,c) and eqn (37a), the following relation must be satisfied at the wave front:

$$\sigma_{r\theta}(\rho_f,\xi) = -m\sigma_{\theta z}(\rho_f,\xi) \tag{53b}$$

from which

$$\sigma_{n\theta} = M\sigma_{\theta z}. \tag{53c}$$

Substituting in eqn (52), we obtain finally the condition

$$\left[-\frac{\mu}{a}s\bar{v} - \bar{\sigma}_{\theta z}\right] = 0. \tag{54}$$

From the relation of eqn (21b), we conclude that the Rankine–Huginiot relation is satisfied.

4. SOLUTION:SUBSEISMIC CASE, $V/c_s < 1$.

For the subseismic case, which corresponds to eqn (12) with $m^2 < 0$, the response for $\xi < 0$ is not quiescent and no sharp front can exist. Consequently, the use of the Laplace transform is

precluded and for this case, the Fourier transform

$$\hat{f}(\omega) = \mathscr{F}[f(\xi)] = \frac{1}{\sqrt{(2\pi)}} \int_{-\infty}^{\infty} f(\xi) e^{i\omega\xi} d\xi \tag{55a}$$

with inversion

$$f(\xi) = \frac{1}{\sqrt{(2\pi)}} \int_{-\infty}^{\infty} \hat{f}(\omega) e^{-i\omega\xi} d\omega \tag{55b}$$

is used.

Application of the transform to eqn (12) yields

$$\frac{\partial^2 \hat{v}}{\partial \rho^2} + \frac{1}{\rho} \frac{\partial \hat{v}}{\partial \rho} - (q^2 \omega^2 + 1/\rho^2) \hat{v} = 0 \tag{56}$$

where

$$q^2 = -m^2 = 1 - M^2 > 0. \tag{57}$$

The non-zero transformed stresses throughout the medium, from eqn (15), are then

$$\hat{\sigma}_{r\theta} = \frac{\mu}{a} \left(\frac{\partial \hat{v}}{\partial \rho} - \frac{\hat{v}}{\rho} \right) \tag{58a}$$

$$\hat{\sigma}_{\theta z} = -\frac{i\mu\omega}{a} \hat{v} \tag{58b}$$

and consequently, the transformed boundary condition, from eqn (16), becomes

$$\frac{d\hat{v}}{d\rho} - \frac{\hat{v}}{\rho} \bigg|_{\rho=1} = \frac{P}{\mu\sqrt{(2\pi)}}. \tag{59}$$

Noting that ω is defined in the range $-\infty < \omega < \infty$ and recalling from eqn (33) that (with $x > 0$)

$$\lim_{x \to \infty} Im\{K_n(-x)\} = \pm \pi \lim_{x \to \infty} I_n(x) \to \pm\infty, \tag{60}$$

solutions of eqn (56) which decay as $\rho \to \infty$ are then

$$\hat{v}(\rho,\omega) = A(\omega) \, \mathrm{Re}\{K_1(q\omega\rho)\}. \tag{61}$$

For $\omega > 0$, substitution in the boundary condition, eqn (59) yields, as in the superseismic case, the constant $A(\omega)$. Proceeding, as in the superseismic case, the desired transformed quantities become:

$$\hat{v}(\rho,\omega) = \frac{-P}{\sqrt{(2\pi)}\, q\omega\mu} \frac{K_1(q\omega\rho)}{K_2(q\omega)} \tag{62a}$$

$$\hat{\sigma}_{r\theta}(\rho,\omega) = \frac{P}{\sqrt{(2\pi)}\, a} \frac{K_2(q\omega\rho)}{K_2(q\omega)} \tag{62b}$$

$$\hat{\sigma}_{\theta z}(\rho,\omega) = \frac{iP}{\sqrt{(2\pi)}\, qa} \frac{K_1(q\omega\rho)}{K_2(q\omega)}. \tag{62c}$$

For $\omega < 0$, following a similar procedure, the transform quantities are

$$\hat{v}(\rho,\omega) = -\frac{P}{\sqrt{(2\pi)}\, q\omega\mu} \frac{K_1(q|\omega|\rho)}{K_2(q|\omega|)} \tag{63a}$$

$$\hat{\sigma}_{r\theta}(\rho,\omega) = \frac{P}{\sqrt{(2\pi)}\,a} \frac{K_2(q|\omega|\rho)}{K_2(q|\omega|)} \tag{63b}$$

$$\hat{\sigma}_{\theta z}(\rho,\omega) = -\frac{iP}{\sqrt{(2\pi)}\,qa} \frac{K_1(q|\omega|\rho)}{K_2(q|\omega|)} \tag{63c}$$

Comparing eqns (62) and (63), we observe that the displacement $\hat{v}$ and the stress $\hat{\sigma}_{r\theta}$ are even functions of ω while $\hat{\sigma}_{\theta z}$ is an odd function of ω. Consequently, the final inversion for these quantities for all ξ and $1 < \rho$ are given by

$$\frac{\mu v}{P}(\rho,\xi) = -\frac{1}{\pi q} \int_0^\infty \frac{K_1(q\omega\rho)}{K_2(q\omega)} \cos \omega\xi \, d\omega \tag{64a}$$

$$\frac{a\sigma_{r\theta}}{P}(\rho,\xi) = \frac{1}{\pi} \int_0^\infty \frac{K_2(q\omega\rho)}{K_2(q\omega)} \cos \omega\xi \, d\omega \tag{64b}$$

$$\frac{a\sigma_{\theta z}}{P}(\rho,\xi) = \frac{1}{\pi q} \int_0^\infty \frac{K_1(q\omega\rho)}{K_2(q\omega)} \sin \omega\xi \, d\omega. \tag{64c}$$

At this stage, the desired quantities are expressed in terms of real indefinite integrals while in the superseismic case the integrals, eqns (27), were over complex quantities. Moreover, while in the previous case, contour integration yielded the specific behavior at the wave front, for the sub-seismic case at hand no such information can be expected. Furthermore, since a numerical integration of the branch integrals is required in any case if contour integration is performed, any advantage to extending the integration to the complex plane is vitiated. Noting thus that no particular benefit is to be gained here by contour integration, the above integrals appearing in eqns (64) are evaluated numerically. Results presented below have been evaluated in this manner.

5. THE LIMITING CASE $V = c_s$, $M = 1$

The solution for the case where the load travels with the velocity $V = c_s$ is a limiting case and may be obtained simply. Since, again, the medium is clearly quiescent for $\xi < 0$, the Laplace transform is applicable and the basic equations of the superseismic case remain valid. Equations (20)–(22) remain unchanged, and setting $m^2 = M^2 - 1 = 0$, eqn (20) becomes

$$\frac{\partial^2 \bar{v}}{\partial \rho^2} + \frac{1}{\rho} \frac{\partial \bar{v}}{\partial \rho} - \frac{\bar{v}}{\rho^2} = 0. \tag{65}$$

Solutions of eqn (65) which decay as $\rho \to \infty$ are

$$\bar{v}(\rho, s) = \frac{A(s)}{\rho}. \tag{66}$$

Substituting in the boundary condition, eqn (22), $A(s)$ is evaluated as before and it follows that

$$\bar{v}(\rho,s) = -\frac{P}{2\mu\rho}. \tag{67}$$

Then, from eqn (21a),

$$\bar{\sigma}_{r\theta}(\rho,s) = \frac{P}{a\rho^2}. \tag{68}$$

The inversions are found, by inspection, to be

$$v(\rho,\xi) = -\frac{P}{2\mu\rho} \delta(\xi) \tag{69}$$

and

$$\sigma_{r\theta}(\rho,\xi) = \frac{P}{a\rho^2}\,\delta(\xi) \tag{70}$$

From eqn (15b)

$$\sigma_{\theta z}(\rho,\xi) = \frac{\mu}{a}\frac{\partial v}{\partial \xi} = -\frac{P}{2\mu\rho}\frac{d[\delta(\xi)]}{d\xi}. \tag{71}$$

Thus we note that for this limiting case, the displacements and stresses in the medium are everywhere zero except along the line $\xi = 0$, (Fig. 4). Along this line the displacements and stresses $\sigma_{r\theta}$ behave as a Dirac-delta function while $\sigma_{\theta z}$ behaves as a doublet; all quantities decay rapidly as $\rho \to \infty$.

It is of interest to observe from this solution that if a step (torsional) load travels with velocity $V = c_s$ along the bore, the displacements and stresses throughout the medium are

$$v(\rho,\xi) = -\frac{P}{2\mu\rho}\,H(\xi) \tag{72a}$$

$$\sigma_{r\theta}(\rho,\xi) = \frac{P}{a\rho^2}\,H(\xi) \tag{72b}$$

$$\sigma_{\theta z}(\rho,\xi) = -\frac{P}{2a\rho}\,\delta(\xi) \tag{72c}$$

where $H(\xi)$ is the unit step function.

The displacements v and stresses $\sigma_{r\theta}$, as expected, are identical with the static behavior of a medium subjected to a uniform torsion load applied along the entire bore.

6. NUMERICAL RESULTS AND CONCLUSIONS

Numerical results for the displacements and stresses throughout the medium are presented for typical superseismic and subseismic cases in Figs. 5–8 and Figs. 9–11 respectively.

Results for the superseismic case with $M = 2$ were calculated from the expressions of Section 3. In Fig. 5, the circumferential displacements are presented as a function of the radial coordinate ρ for a family of curves ξ representing the longitudinal distance behind the line of applied loading. It is observed, in all cases, that the largest displacement occurs in the vicinity behind the wave front and decreases for points approaching the cavity boundary, $\rho = 1$. For distances far behind the point of applied loading, the displacements also decay. The peak displacements, which occur at the wave front, are found to be equal to the jump at the wave front (see eqn 48),

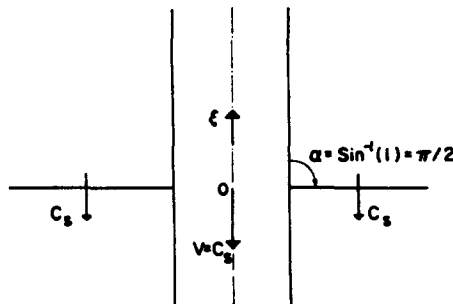$$\left[\frac{\mu v}{P}\right] = -\frac{1}{m}\sqrt{(1/\rho_f)}. \tag{73}\dagger$$

Fig. 4. Limiting case, $M = V/c_s = 1$.

†The jump $[v]$ as given here represents $[v] = v(\rho_f^+) - v(\rho_f^-) = v(\rho_f^-)$ since $v(\rho_f^+) = 0$ ahead of the front.
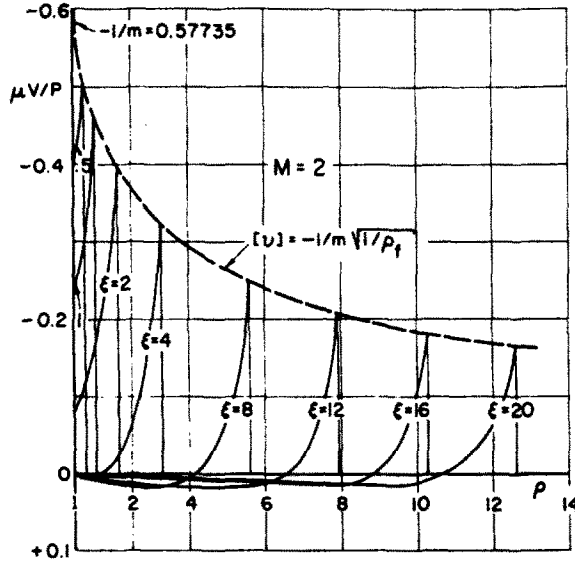
Fig. 5. Typical superseismic case ($M = 2$): displacements behind wave front.

The locus of these peaks is shown in Fig. 5 by the broken curve. Thus, eqn (73) provides a simple algebraic expression for calculating the peak curve for any given Mach number M.†

The stress components $\sigma_{r\theta}$ are presented in Fig. 6 as a function of the radial coordinate for various values of ξ. The peak stresses again occur immediately behind the wave front and decay to zero at $\rho = 1$ for all $\xi > 0$. It is of interest to observe that the largest stresses occur at the wave front in the vicinity of $\xi = 3$. Furthermore, for relatively small values of ξ, $0 < \xi < 1$, the $\sigma_{r\theta}$ stresses vary almost linearly with ρ. However, for relatively large ξ, $8 > \xi$, the stresses are infinitesimally small for distances far behind the wave front while remaining significantly large in the vicinity of the wave front.

A similar behavior is seen to occur for the stress components $\sigma_{z\theta}$ as presented in Fig. 7. It is noted that these stresses do not vanish at $\rho = 1$.

The effect of the variation of the Mach number M is shown in Fig. 8 where the displacement at the cavity boundary $\rho = 1$ is presented for three values, $M = 1.1, 2$ and 4, as a function of ξ. In all cases, the displacements tend to zero as ξ becomes large. As M approaches unity (i.e. $M = 1.1$) the predominant displacements at the boundary are seen to occur in the vicinity of the applied load. In fact as $M \to 1$, the displacement is represented by the Dirac-delta function as
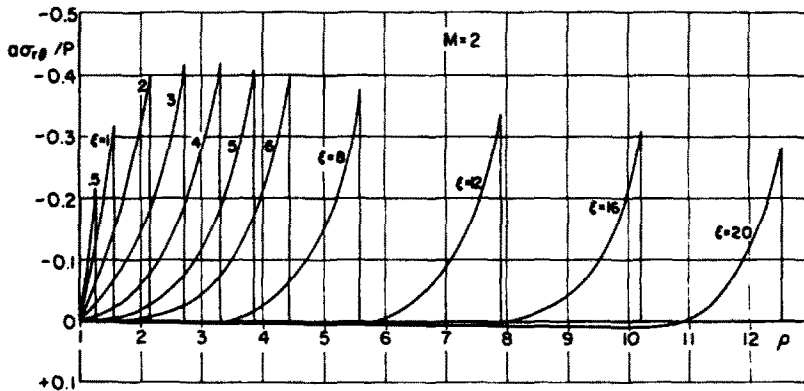

Fig. 6. Typical superseismic case ($M = 2$): stress components $\sigma_{r\theta}$.

†The displacements of all points, $1 \le \rho \le \rho_f$, were calculated using eqns (30) and (34a) according to the numerical scheme described in Appendix A. The peak displacements at $\rho = \rho_f$, thus calculated, were found to be identical (to six significant figures) to the value given by eqn (73). This, in effect provided an excellent verification on the accuracy of the numerical scheme.
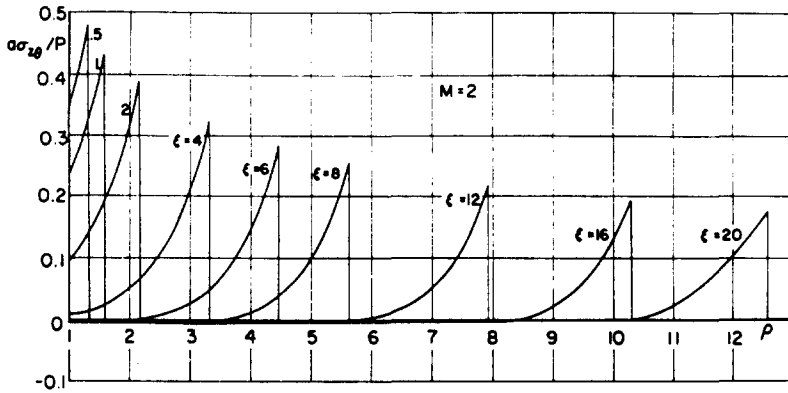
Fig. 7. Typical superseismic case $(M = 2)$: stress components $\sigma_{z\theta}$.

was shown in the limiting case (eqn 69). It is noted also, from Fig. 8 that as M increases, the displacements decrease monotonically.

Typical results for the subseismic case are given for a value $M = 0.5$ and are shown in Figs. (9–11) as a function of the radial coordinate, $1 < \rho$.

For the subseismic case, no sharp wave front exists and the character of the response is seen to be entirely different from that of the superseismic case. The behavior is observed to vary smoothly and to decay rapidly with both ρ and ξ coordinates.

Results presented were obtained by evaluation of eqns (64) of Section 4 following the numerical scheme given in Appendix B.

In Fig. 9, the displacements are presented for several values of ξ. At $\xi = 0$, the maximum displacement occurs at the cavity boundary and decays rapidly and monotonically with the radial coordinate. However, while the displacement is observed to decay rapidly with ξ, for increasing values of ξ, relative peaks are seen to occur at increasing larger radial distances from the cavity axis.

The behavior of the stresses $\sigma_{r\theta}$ and $\sigma_{\theta z}$ are given in Figs. 10 and 11. The stresses are observed to have a behavior similar to the displacement. In general it is possible to conclude that, in contrast to the superseismic case, in the subseismic case the medium is excited
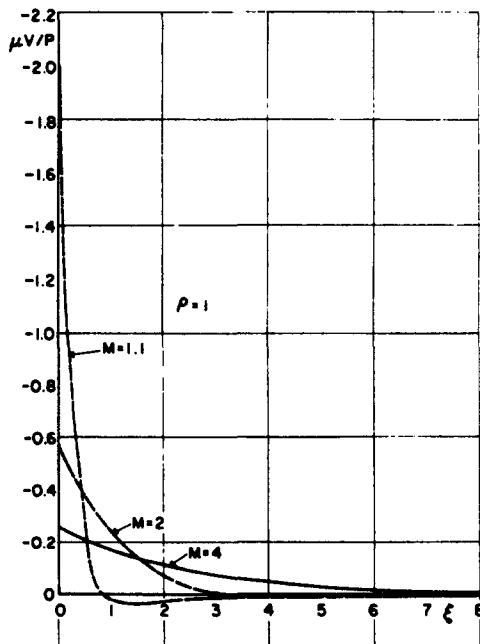

Fig. 8. Superseismic case: effect of Mach number on displacements at $\rho = 1$.
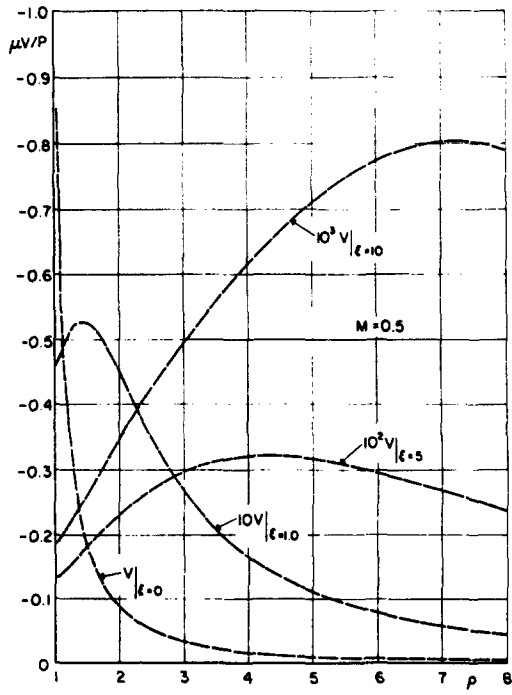
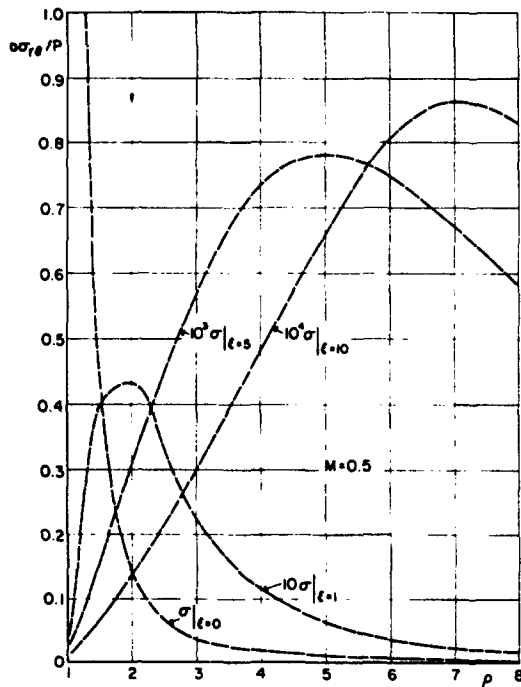Fig. 9. Typical subseismic case ($M = 0.5$): displacements.

Fig. 10. Typical subseismic case ($M = 0.5$): stress components $\sigma_{r\theta}$.
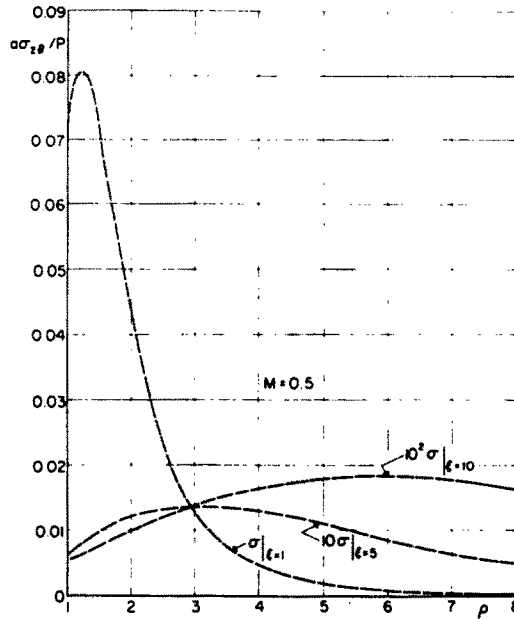
Fig. 11. Typical subseismic case ($M = 0.5$): stress components $\sigma_{z\theta}$.

predominantly in the vicinity of the local points of application of the applied load and exhibits a behavior which decays with the radial coordinate both ahead and behind the position of the load.

REFERENCES

1. L. Frýba, *Vibration of Solids and Structures under Moving Loads.* Noordhoff, Groningen (1972).
2. I. N. Sneddon, Stress produced by a pulse of pressure moving along the surface of a semi-infinite solid. *Rendiconti Circolo Matematico di Palermo,* 2, 57–62 (1952).
3. J. Cole and J. Huth, Stresses produced in a half plane by moving loads *J. Appl. Mech.* 25(4), 433–436 (1958).
4. R. Parnes, Response of an infinite elastic medium to traveling loads in a cylindrical bore *J. Appl. Mech.* 36(1), 51–58 (March 1969).
5. R. Parnes, Complex zeros of the modified Bessel functions $K_n(z)$. *Math. of Comput.* 26(120), 949–953 (Oct. 1972).
6. N. W. McLachlan, *Bessel Functions for Engineers,* 2nd Edn Oxford University Press, Oxford (1955).
7. M. A. Abramowitz and I. A. Stegun, *Handbook of Mathematical Functions.* Dover, New York (1964).
8. A. R. Forsyth, *Theory of Functions of a Complex Variable,* 3rd Edn. Vol. 1. Dover, New York (1965).
9. I. N. Sneddon, *Fourier Transforms.* McGraw-Hill, New York (1951).
10. R. Parnes and E. R. Johnson, Propagation of axisymmetric waves in an elastic half-space containing a cylindrical inclusion—Part II Analysis of singularities, behavior at wave fronts and numerical results. *Quart. J. Mech. Appl. Math.* 30, 255–268 (Aug. 1977).
11. D. R. Bland, *Nonlinear Dynamic Elasticity.* Blaisdell, New York (1969).

APPENDIX A

Evaluation of branch integrals. Superseismic case

The branch integrals appearing in eqns (34) contain integrands of the form

$$\Phi_{n,k}(m\zeta,\rho) = \frac{G_n(m\zeta,\rho)}{\zeta^k D(m\zeta)}e^{-\zeta t}, \quad n = 1,2; \ k = 0,1 \tag{A.1}$$

which, because of their complexity, must be integrated numerically over the range $0 \leq \zeta < \infty$. However, recognizing that the above quantities represent ratios of the K_n and I_n Bessel functions, it is possible to separate the infinite range into two regions, $0 < \zeta < \zeta_0$, and $\zeta_0 < \zeta < \infty$, such that in the second region the integrals can be integrated asymptotically. To this end, let the various integrals appearing in eqn (34) be written as

$$S_{n,k} = S_{n,k}^{(1)} + S_{n,k}^{(2)} \tag{A.2a}$$

where

$$S_{n,k}^{(1)} = \int_0^{\zeta_0} \Phi_{n,k}(m\zeta,\rho) \, d\zeta \tag{A.2b}$$

$$S_{n,k}^{(2)} = \int_{\zeta_0}^{\infty} \Phi_{n,k}(m\zeta,\rho) \, d\zeta \tag{A.2c}$$

and where ζ_0 is a prescribed finite value of ζ. The finite integrals $S_{n,k}^{(1)}$ are then integrated by an appropriate numerical

scheme (e.g. Simpson's Method). If ζ_0 is chosen sufficiently large, then the K_n and I_n Bessel functions can be represented by the series

$$K_n(z) \sim \sqrt{\left(\frac{\pi}{2z}\right)} e^{-z} [1 + a_n/z + b_n/z^2 + \ldots]$$ (A.3a)

$$I_n(z) \sim \frac{e^z}{\sqrt{(2\pi z)}} [1 - a_n/z + b_n/z^2 + \ldots]$$ (A.3b)

where a_n and b_n are given by eqn (36b).

Retaining the first three terms in each series, and substituting from eqns (35), the asymptotic representation of $\Phi_{n,k}$ for $m\zeta \gg 1$, after algebraic manipulation, is given by

$$\Phi_{n,k}(m\zeta,\rho) = \frac{e^{-2m\zeta}}{\pi\zeta^2\sqrt{(\rho)}} \{ e^{[m(\rho-1)-\xi]\zeta} [1 + k_{n1}/m\zeta + k_{n2}/(m\zeta)^2]$$
$$+ e^{-[m(\rho-1)-\xi]\zeta} [1 + k_{n3}/m\zeta + k_{n4}/(m\zeta)^2] \}$$ (A.4)

where

$$k_{11}(\rho) = 3(15 - 1/\rho)/8, \qquad k_{12} = 2145/128 - 135/64\rho - 15/128\rho^2$$
$$k_{13}(\rho) = 3(5 + 1/\rho)/8, \qquad k_{14} = 345/128 + 45/64\rho - 15/128\rho^2$$
$$k_{21}(\rho) = 285(1 - 1/\rho)/32, \qquad k_{22} = 2145/128 - 675/64\rho + 105/128\rho^2$$
$$k_{22}(\rho) = 165(1 - 1/\rho)/32, \qquad k_{24} = 345/128 + 225/64\rho + 105/128\rho^2.$$ (A.5)

Upon substituting eqn (A.4) in eqn (A.2c), the integrals, evaluated term by term, can be expressed in terms of the integral exponential function[7]

$$E_1(x) = \int_x^\infty \frac{e^{-\eta}}{\eta} d\eta.$$ (A.6)

The final results for the branch integrals $I^{(2)}_{B()}$, $(\zeta_0 < \zeta < \infty)$ are given as follows:

$$I^{(2)}_{B(r)} = -\frac{2\pi i}{m} S^{(2)}_{1,1}$$

$$= -\frac{2i}{m\sqrt{(\rho)}} \left\{ \frac{1}{m\zeta_0}[k_{11} + k_{12}(\zeta_0 - \beta_1)/2\zeta_0 m] e^{-\beta_1\zeta_0} + \left[1 - \frac{k_{11}\beta_1}{m} + \frac{k_{12}\beta_1^2}{2m^2}\right] E_1(\beta_1\zeta_0) \right.$$
$$\left. + \frac{1}{m\zeta_0}[k_{13} + k_{14}(\zeta_0 - \beta_2)/2\zeta_0 m] e^{-\beta_2\zeta_0} + \left[1 - \frac{k_{13}\beta_2}{m} + \frac{k_{14}\beta_2^2}{2m^2}\right] E_1(\beta_2\zeta_0) \right\}$$ (A.7a)

$$I^{(2)}_{B(r\theta)} = 2\pi i S^{(2)}_{1,0}$$

$$= \frac{2i}{\sqrt{(\rho)}} \left\{ \left[\frac{1}{\beta_1} + \frac{k_{22}}{m^2\zeta_0}\right] e^{-\beta_1\zeta_0} + \frac{1}{m}\left[k_{21} - \frac{k_{12}\beta_1}{m}\right] E_1(\beta_1\zeta_0) \right.$$
$$\left. - \left[\frac{1}{\beta_2} + \frac{k_{24}}{m^2\zeta_0}\right] e^{-\beta_2\zeta_0} - \frac{1}{m}\left[k_{22} - \frac{k_{24}\beta_2}{m}\right] E_1(\beta_2\zeta_0) \right\}$$ (A.7b)

$$I^{(2)}_{B(z\theta)} = \frac{2\pi i}{m} S^{(2)}_{1,0}$$

$$= -\frac{2i}{m\sqrt{(\rho)}} \left\{ \left[\frac{1}{\beta_1} + \frac{k_{12}}{m^2\zeta_0}\right] e^{-\beta_1\zeta_0} + \frac{1}{m}\left[k_{11} - \frac{k_{12}\beta_1}{m}\right] E_1(\beta_1\zeta_0) \right.$$
$$\left. + \left[\frac{1}{\beta_2} + \frac{k_{14}}{m^2\zeta_0}\right] e^{-\beta_2\zeta_0} + \frac{1}{m}\left[k_{13} - \frac{k_{14}\beta_2}{m}\right] E_1(\beta_2\zeta_0) \right\}$$ (A.7c)

where, in the above

$$\beta_1 = \xi - m(\rho - 1) + 2m$$
$$\beta_2 = \xi + m(\rho - 1) + 2m.$$ (A.8)

APPENDIX B

Evaluation of the Fourier transform inversions: Subseismic case

From eqns (64), it is observed that the integrals must be integrated over the infinite domain $0 < \omega < \infty$. Proceeding as with the branch integrals of the superseismic case, a prescribed value of ω_0 is chosen such that the range of integration is divided into a finite range $(0 < \omega < \omega_0)$ and an infinite range $(\omega_0 < \omega < \infty)$. In the latter region the integrands are expressed by means of their asymptotic representation. Thus, let the integrals of eqn (64) be written as

$$S_{n,k} = S^{(1)}_{n,k} + S^{(2)}_{n,k}$$ (B.1a)

where

$$S_{n,k}^{(1)} = \int_0^{\omega_0} \psi_{n,k}(q\omega,\rho)\begin{Bmatrix} \cos \omega\xi \\ \sin \omega\xi \end{Bmatrix} d\omega \tag{B.1b}$$

$$S_{n,k}^{(2)} = \int_{\omega_0}^{\tau} \psi_{n,k}(q\omega,\rho)\begin{Bmatrix} \cos \omega\xi \\ \sin \omega\xi \end{Bmatrix} d\omega. \tag{B.1c}$$

In the above

$$\psi_{n,k}(q\omega,\rho) = \frac{K_n(q\omega\rho)}{\omega^k K_2(q\omega)}, \quad n = 1,2; \; k = 0, 1. \tag{B.2}$$

Using the asymptotic expansion for the K_n Bessel functions for $|q\omega| \gg 1$, eqn (A.3a), upon retaining the first few terms, the asymptotic representation of $\psi_{n,k}$ are found to be

$$\psi_{n,k}(q\omega,\rho) = \frac{e^{-(\rho-1)q\omega}}{\omega^k \sqrt{(\rho)}}\left[1 + \frac{\gamma_{n1}}{q\omega} + \frac{\gamma_{n2}}{(q\omega)^2} + \dots\right] \tag{B.3}$$

where

$$\gamma_{11} = -3(5 - 1/\rho)/8, \quad \gamma_{12} = \frac{345}{128} - 45/64\rho - 15/128\rho^2$$

$$\gamma_{21} = -15(1 - 1/\rho)/8, \quad \gamma_{22} = \frac{345}{128} - 225/64\rho + 105/128\rho^2. \tag{B.4}$$

The integrals $S_{n,k}^{(1)}$ are integrated over the finite range $0 < \omega < \omega_0$ using a convenient numerical integration scheme.

The integrals $S_{n,k}^{(2)}$ may be either evaluated analytically term by term or in the case of the displacement an upper bound on the value of $S_{n,k}^{(2)}$ may be established. Performing the integrations, the final results are given as follows

$$\frac{\mu v(\rho,\xi)}{P} = S_{1v}^{(1)} + S_{1v}^{(2)} \quad (n = 1, k = 1) \text{ where} \tag{B.5a}$$

$$|S_v^{(2)}| < \left|\frac{e^{-(\rho-1)q\omega_0}}{\pi q\omega_0 \sqrt{(\rho)}}\frac{1}{\Lambda}[(\rho-1)q \cos \omega_0\xi - \xi \sin \omega_0\xi]\right|, \tag{B.5b}$$

$$\frac{a\sigma_{r\theta}(\rho,\xi)}{P} = S_{r\theta}^{(1)} + S_{r\theta}^{(2)} \quad (n = 2, k = 0) \text{ where} \tag{B.6a}$$

$$S_{r\theta}^{(2)} = \frac{e^{-(\rho-1)q\omega_0}}{\pi\sqrt{(\rho)}}\frac{1}{\Lambda}[(\rho-1)q \cos \omega_0\xi - \xi \sin \omega_0\xi](1 + R_{r\theta}). \tag{B.6b}$$

$$\frac{a\sigma_{\theta z}(\rho,\xi)}{P} = S_{\theta z}^{(1)} + S_{\theta z}^{(2)} \quad (n = 1, k = 0) \text{ where} \tag{B.7a}$$

$$S_{\theta z}^{(2)} = \frac{e^{-(\rho-1)q\omega_0}}{\pi q\sqrt{(\rho)}}\frac{1}{\Lambda}[(\rho-1)q \sin \omega_0\xi + \xi \cos \omega_0\xi](1 + R_{\theta z}), \tag{B.7b}$$

where, in the above

$$\Lambda = (\rho - 1)^2 q^2 + \xi^2 \tag{B.8}$$

and the remainders are

$$R_{r\theta} < 15/(1 - 1/\rho)/8q\omega_0 \tag{B.9a}$$

$$R_{\theta z} < (15 - 3/\rho)/8q\omega_0. \tag{B.9b}$$

It is noticed, from eqns (B.9) that it is always possible to obtain an estimate of the upper bound on the remainder (which arises from retention of only the first terms of the asymptotic expansions). An appropriate choice of ω_0 will thus give a prescribed accuracy to the solution.